SIMULATION, DEVELOPMENT, AND FIELD MEASUREMENT VALIDATION OF AN ISOLATION SYSTEM FOR A NEW ELECTRONICS CABINET IN THE SPACE SHUTTLE LAUNCH ENVIRONMENT WITHIN THE MOBILE LAUNCH PLATFORM

by

Alan R. Klembczyk, Chief Engineer
Taylor Devices, Inc.
90 Taylor Drive
North Tonawanda, NY 14120-0748

Michael W. Mosher, Engineering Manager
Carleton Technologies, Inc.
Orchard Park, NY

SIMULATION, DEVELOPMENT, AND FIELD MEASUREMENT VALIDATION OF AN ISOLATION SYSTEM FOR A NEW ELECTRONICS CABINET IN THE SPACE SHUTTLE LAUNCH ENVIRONMENT WITHIN THE MOBILE LAUNCH PLATFORM

Alan R. Klembczyk, Chief Engineer
Taylor Devices, Inc.
North Tonawanda, NY 14120-0748
716-694-0800

Michael W. Mosher, Engineering Manager
Carleton Technologies, Inc.
Orchard Park, NY

Recent replacement of the cabinet-mounted low voltage power switchgear within the Space Shuttle Mobile Launch Platform (MLP) has necessitated the need for a dynamic analysis and the development of a 6 degree of freedom isolation system. This is required due to the addition of electronic sensing and control components in modern electronic switchgear and the harsh vibration environment experienced within the MLP during a launch of the Shuttle. The isolation system is required to isolate the switchgear to prevent the spurious tripping of breakers that would compromise Programmable Logic Control (PLC) operation during launch. An added benefit of the isolation system is that it provides vibration isolation during the Shuttle's approximately three mile journey between the Vehicle Assembly Building (VAB) and either of its two launch pads. Initially, a broadband launch environment PSD input was defined. Then, a 3-dimensional dynamic analysis was performed in 6 degrees of freedom in order to optimize the isolation system attributes including parametric output and mounting arrangement within the existing structure. The isolation system was then designed, built, and integrated within the MLP after making some structural modifications to the MLP support steel. Finally, broadband dynamic measurements were made during an actual Shuttle launch in order to verify the effectiveness of the isolation system and to validate the predictions of the analysis. Measurements made during the launch of STS-115 on September 9, 2006, have affirmed the effectiveness and the predicted performance of the isolation system.

INTRODUCTION

During the development stage of the Space Shuttle during the 1970's, some of the ground support equipment (GSE) remaining from the Apollo program was earmarked for use on the new Program to save cost and to retain a proven design capable of supporting a variety of launch payloads.

Apollo 11 1969

STS-1 1980

Figure 1: MLP Supporting Saturn V of the Apollo Program and the Space Shuttle

One example of this is the Mobile Launch Platform (MLP) that supported vehicles of both Programs. Figure 1 illustrates both the Saturn V rocket of the Apollo Program and the Space Shuttle supported on the MLP for transportation and launch operations. Three of these structures exist today that support the Shuttle Program, one of which is intended for use on the next generation of launch vehicles.

During development of the Shuttle, electronic switchgear was integrated within the MLP to control various functions requiring electronic power during launch. For more than 25 years, this switchgear was used for more than 100 Shuttle launches. Recently, the aged switchgear required replacement. However, modern electronics design differed to a substantial degree, enough to warrant an examination of the existing isolation system for use on the new switchgear. The previous isolation system consisted of a series of coil springs that were deemed to be unacceptable for current use. Additionally, motion of the old switchgear during transportation was excessive. This required the ground crew to block up the isolation system on rubber pads to avoid risk to the switchgear. This was an undesirable arrangement since the isolation system could otherwise provide a high degree of vibration isolation during transportation to the switchgear if designed accordingly.

As with many dynamic systems under evaluation for shock and/or vibration response and mitigation, it is oftentimes necessary to break down the effort into three main phases: The first is to define the dynamic environment that exists. The second is to define the fragility level of the equipment. The last is to determine whether or not mitigation through isolation or other means is necessary. Additionally, this final phase requires that the isolation system parameters be defined through analysis or test as necessary. For the current effort, the dynamic environment was defined by direct measurement. The fragility level was defined by component survivability through a standard vibration test previously performed on the switchgear. The isolation system parameters were defined by optimization of a 6 degree of freedom model as outlined within this paper. Finally, the effectiveness of the isolation system was verified by measurement during an actual Shuttle launch.

DEFINITION OF DYNAMIC ENVIRONMENT AND MITIGATION GOAL

The response during launch of the floor of the MLP that supports the switchgear was captured using accelerometers in the vertical direction during a recent Shuttle mission and then converted into the form of a power spectral density (PSD). This was to be used as the input, or the dynamic environment, to which the system was to be analyzed.

The response mitigation goal (fragility level) was to reduce the cabinet accelerations to below the component level vibration environment that the switchgear was qualified to originally (by test) in terms of g's versus time. This was provided by the switchgear manufacturer that performed the tests. In this case, failure is partially defined as the ability to avoid any spurious tripping of the breakers within the switchgear since this would compromise the PLC logic necessary for proper operation during launch. Since the equipment was able to pass the component vibration test without failure, it is unknown as to what the maximum possible amplitude the equipment can survive before failure occurs (energy distribution over frequency or maximum acceleration level in time, etc.). Therefore, the isolation system was required to mitigate the input to a level below the maximum acceleration level the equipment was subjected to in the component test, which in this case was 0.50 g_{rms}.

ANALYTICAL MODEL DESCRIPTION

A simple single degree-of-freedom (SDOF) model was used initially in order to make a preliminary estimate of the possible input mitigation that could be obtained at the switchgear given the constraints on the system using an isolation system consisting of a series of springs and dampers. These constraints were the height of the switchgear cabinet, the height of the elements used in the isolation system, and the total amount of cabinet travel all relative to the available height within the MLP. The weight of the switchgear is approximately 26,000 lbs. that includes suspended electronic cabling required for the system.

The initial SDOF model showed that a rather large amount of damping was necessary to reduce the required travel to a desired value of ±4.5 inches using the given MLP PSD input. This resulted in large payload accelerations due to the transmission of the higher frequency content of the input. This was a rather large excursion given the relatively short duration of the launch event. It was then determined that a reduction of the low frequency portion (up to 20 Hz) of the PSD should be applied given that the provided PSD is stationary, yet the actual event is non-stationary. The entire event is less than 10 seconds. Thus, the low frequency content was most likely overestimated,

affecting the resulting isolation system travel. The recalculated input spectrum (PSD) was then used as the input to the model. Both are shown in Figure 2. Knowing that the switchgear cabinet excitation is in all three translational directions and that the input was recorded only in the vertical direction, the input is assumed to be of equivalent magnitude in all three orthogonal axes due to the lack of test data. This also is believed to be conservative.

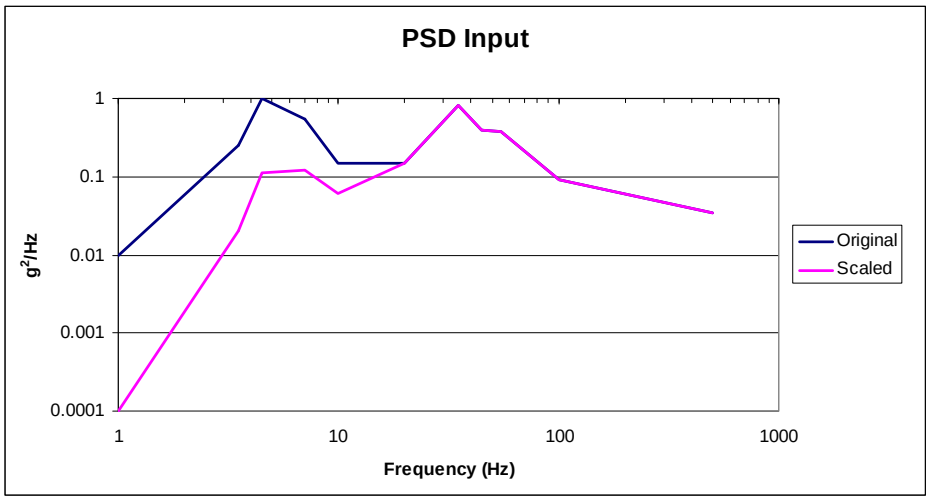

Figure 2: Switchgear Input (7.1 g_{rms}) and Scaled PSD Profiles (6.8 g_{rms})

Given the nature of the geometry of the switchgear cabinet, its size, and the fact that the input is present in some unknown level in all three orthogonal directions, the isolation system was to be able to provide isolation in all three translational directions. This meant that the isolation system had to account for all the cabinet's six rigid body modes (three translational and three rotational). Given the large length and height dimensions with respect to the width as shown in Figures 3 and 4, the mount deflections at the corner of the cabinets could possibly be higher with respect to the motion of the center of gravity of the payload by the additive nature of the roll mode (rotation about X, the longest cabinet axis) of the cabinet.

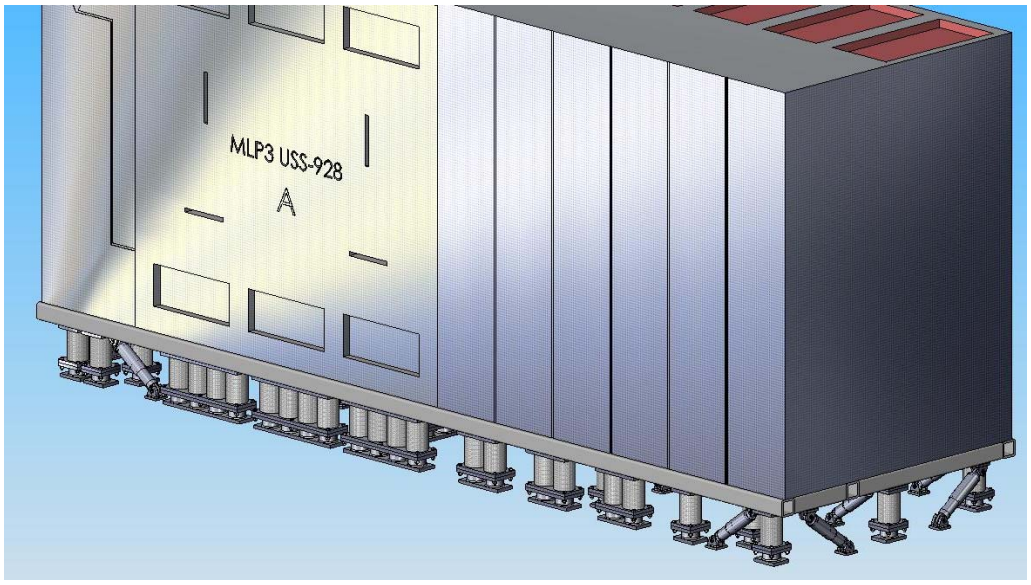

Figure 3: Isometric View of Switchgear Cabinet Including Final Isolation System

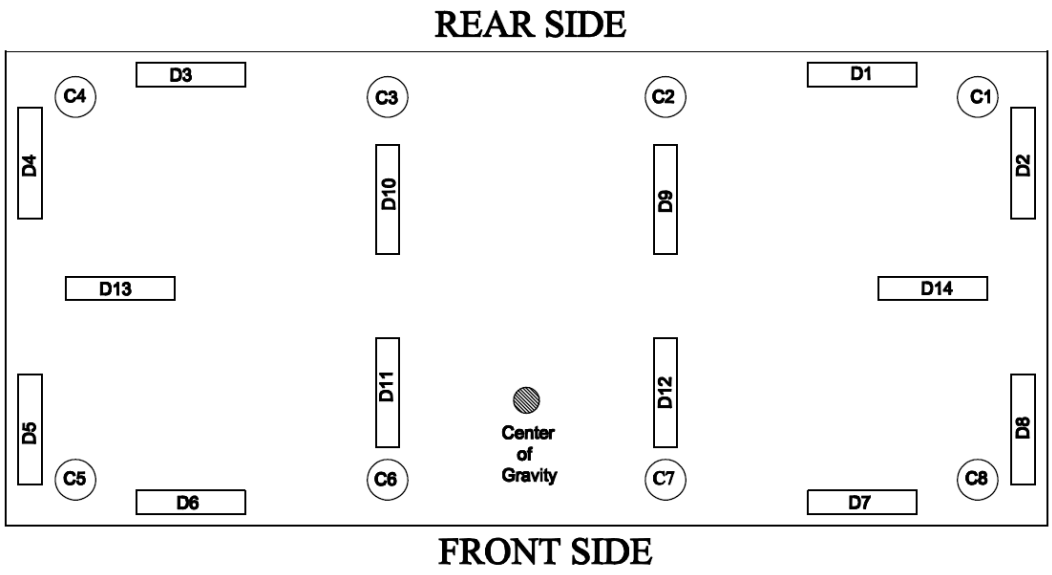

Figure 4: Top View of Lumped Isolator Configuration Used in Model

X: the axis of the cabinet along the long side of the cabinet
Y: the axis of the cabinet along the short side of the cabinet
Z: the vertical axis
θx: roll axis
θy: pitch axis
θz: yaw axis

The analytical model of the system used eight lumped spring locations, four across the front and back of the cabinet as shown in Figure 4. This was done to keep computer run times to a minimum without losing model accuracy. Each lumped spring representation is labeled "C" in Figure 4. The actual isolation system was to use more springs for better distribution and hardware constraints (available height for springs) as long as they were placed at the elastic center of the lumped spring packs in the model. Fourteen dampers labeled "D" in Figure 4 were implemented into the model.

An initial modal study attempted to stiffen the rotational modes with the goal of reducing the spring and damper deflections and reducing the effective front-to-back displacement of the cabinet at the center of gravity. This is even larger at the top of the cabinet due to the linear amplification effect that length has on angular motion. However, there is a limitation as to how rigid the rotational mode can be made due to the direct coupling with the vertical direction since spring stiffness and damping in the vertical direction has the most effect on the roll motion.

Eventually, the modeling effort had to be performed in the time domain to include the effect of the overturning moments induced by gravity acting on the center of gravity due to the rotation of the cabinet with respect to the base of the cabinet. This is especially true of the roll mode due to the isolation system footprint with respect to the cabinet width and the height dimension of the center of gravity with respect to the isolation plane. This is difficult to capture when using a modal analysis technique (which was run as a check on the transient analysis). Therefore, three time realizations of the PSD were generated to be used as the final input to the system.

The initial 6-DOF study was compared against a SDOF model by matching the vertical natural frequency and damping to that of a SDOF model for three frequencies: 1.5 Hz, 2.5 Hz, 3.5 Hz all at 25% critical damping. The SDOF travel and acceleration (g's) are listed against the 6-DOF model results in Table 1.

	Vertical Frequency (Hz)	1.50	2.50	3.50
SDOF	Travel (in)	1.20	1.20	1.75
	G's	0.50	1.50	2.50
6 DOF	Z Travel (in)	2.04	1.33	1.31
	Dynamic Mount Deflection (in)	4.30	2.90	2.69
	Z (G's)	0.50	1.20	2.10
	Roll (Hz)	0.90	1.50	2.00

Table 1: Comparison of SDOF Results to the 6-DOF Analysis

Reviewing the results of the SDOF model summarized in Table 1, it can be observed that the travel increases with increasing frequency. This appears to be counter-intuitive. However, the increase in the model frequency actually shifts the natural frequency of the system into a region of increasing energy content in the provided spectrum shown in Figure 2. This is a topic of a discussion later in the paper regarding the conservatism of the low frequency input PSD. Also worth noting is the roll mode stiffens at a rate slightly over one-half the vertical mode. What is not shown are the rather large displacements in the Y direction for the 6-DOF model at the center of gravity of the cabinet in the front-to-back direction (Y axis) of 3.57", 2.21", and 2.19" for the 1.5 Hz, 2.5Hz, and 3.5 Hz vertical system frequencies respectively.

Although the results in the vertical direction for the 6-DOF model are reasonable when compared with the SDOF model, the side-to-side deflections at the center of gravity (at this time assumed to be at the center of geometry) were dominated by the motion due to the low roll mode frequency. This resulted in vertical system travel at the center of gravity of 3.57", 2.21", and 2.19" for vertical system frequencies of 1.5 Hz, 2.5 Hz, and 3.5 Hz respectively. This results in rather large spring and damper displacements at the corners of the cabinets of 4.30", 2.90", and 2.69" for the same vertical system frequencies. The large spring and damper deflections for the 1.5 and 2.5 Hz systems due to the low roll mode frequency, coupled with the rather large static deflections required of these elements under the static weight of the cabinet, made them impossible to fit within the given system constraints.

It was determined the most viable isolation system was one with a system vertical mode of approximately 3.5 Hz with 22% critical damping. This brought the individual isolator parameters into manageable levels while preserving the mitigation goal at the payload. The resulting transfer functions at the center of gravity of the cabinet for the translational and rotational modes are shown in Figure 5 and Figure 6, respectively. Clearly evident in the profiles is the coupling effect of the modes as evidenced by the smaller secondary local peaks in the transfer functions.

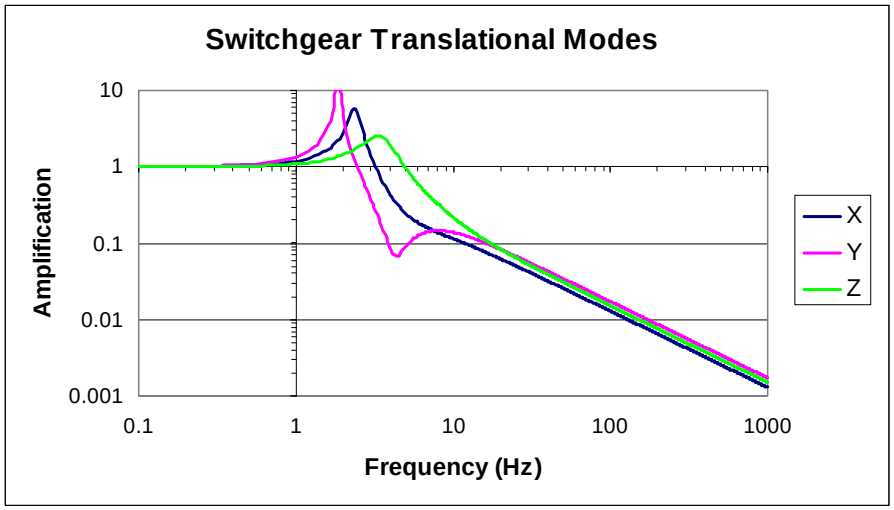

Figure 5: Modal Model Results of Translation Modes

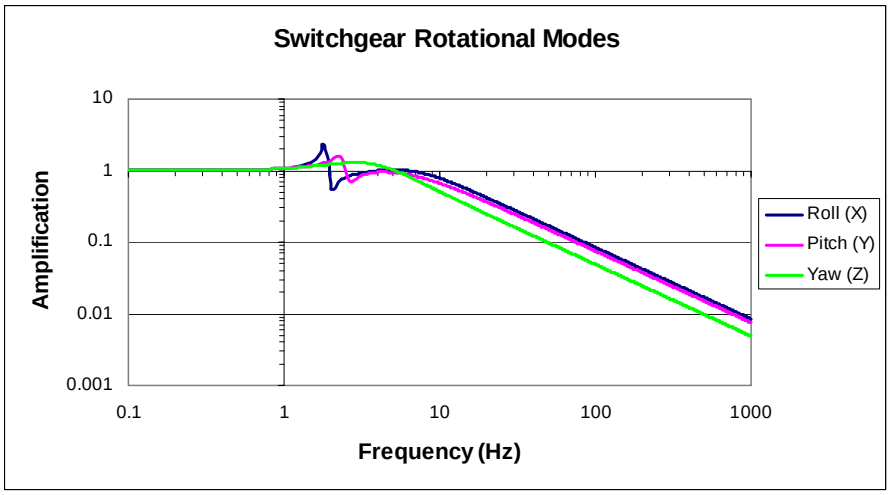

Figure 6: Modal Model Results of Rotational Modes

The final cabinet configuration was established in which the center of gravity was both offset to the back and to a lesser degree to one side, further complicating the influence of the rotational modes on the isolator stroke as well as the translational motion, especially front-to-back, at the top of the cabinet. Also unknown was the effect of unaccounted additional cable weight on the center of gravity location. However, it was assumed it would have a negligible effect due to the fact that the cable represented only approximately 7% of the total system weight. The resulting isolator configuration attempted to balance the cabinet statically such that the cabinet would not be leaning due to its own weight while sitting on the isolators. The solution was to place more isolators at the back of the cabinet to essentially balance the static load on the individual isolators and in turn to improve the balance of the dynamic modes. The center of gravity of the cabinet sits above the isolation plane (the bottom of the cabinet). This causes the roll mode frequency to be a strong contributor to isolator displacement. Therefore, the isolators would need to be located in such a manner that they increase the roll mode as much as possible as well as the effective damping.

The damping is needed to provide approximately 22% critical with respect to the cabinet mass in the vertical direction. The dampers were placed at an angle of 35.3° with the horizontal plane with an included angle of 90° between pairs (a pair is placed at each of the four corners of the cabinet). Since the dampers are uni-axial devices, motions will be coupled due to their orientations, which again supported the reasoning behind performing a transient analysis rather than just a modal analysis. The 35.3° angle from horizontal gives the closest to symmetric damping in the three orthogonal axes.

Table 2 shows the worst case results of the time histories of the translational travel of the cabinet at the center of gravity, the rotation of the cabinet about the center of gravity, the strokes of the springs at the worst case corner deflection, and the opposing corner in all three orthogonal directions, and the damper stroke and output forces.

		X (in)	Y (in)	Z (in)	Roll (θx)	Pitch (θy)	Yaw (θz)
Modal Analysis	Frequency (Hz)	2.40	1.90	3.40	1.80	2.30	2.90
	Q (Magnitude Factor)	5.80	10.00	2.60	2.40	1.60	1.30
System Performance	Static Deflection	0.02	-0.04	-0.80	0.05	0.03	N/A
	Dynamic Deflection	1.78	2.19	1.68	2.06	0.52	N/A
		-1.58	-1.98	-2.09	-1.49	-0.57	N/A
	Payload Response (G's)	1.70	1.30	2.20	N/A	N/A	N/A
		-1.40	-1.30	-2.70	N/A	N/A	N/A
Spring Performance	Static Deflection	N/A	N/A	0.87	N/A	N/A	N/A
	Dynamic Deflection	1.73	1.00	2.80	N/A	N/A	N/A
		-1.38	-0.98	-2.61	N/A	N/A	N/A
Damper Performance	Stroke	1.57	N/A	N/A	N/A	N/A	N/A
		-1.56	N/A	N/A	N/A	N/A	N/A
	Force (lb)	9,963	N/A	N/A	N/A	N/A	N/A

Table 2: Overall Analytical Results (Worst case amplitudes over the three realizations)

It should be noted the required translational motion of the cabinet at the top would include both the translational motion at the center of gravity as well as the contribution of the angular displacement of the cabinet about the center of gravity, multiplied by the distance from the center of gravity to the particular point at the top. The motions in the horizontal directions required at the top will be greater than that required at the isolation base since the cabinet will pitch and roll. The results of the transient analysis were compared against the modal analysis results to gain confidence in the modeling by converting the resulting time histories to PSD's and comparing them against the resulting PSD's generated by passing the spectral input through the resulting frequency response functions. The results were extremely close as shown in figures 7-9 for each of the translational axes.

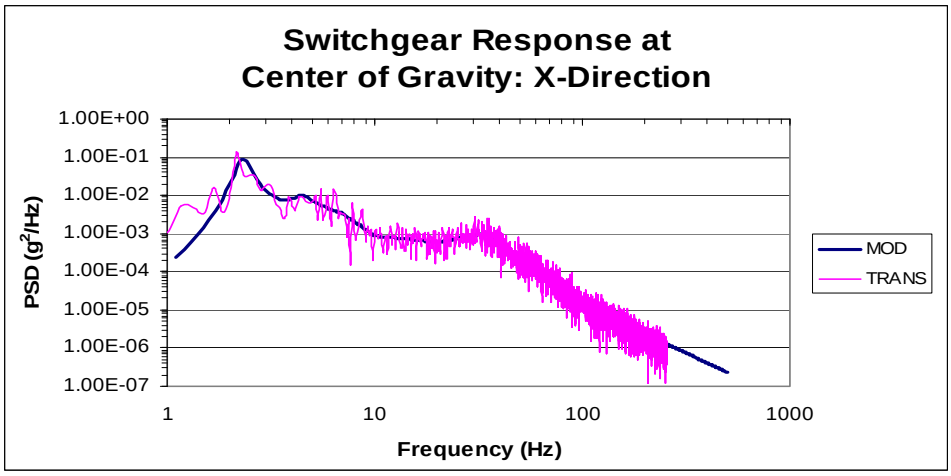

Figure 7: Transient Model vs. Modal Model in X (0.34 g_{rms})

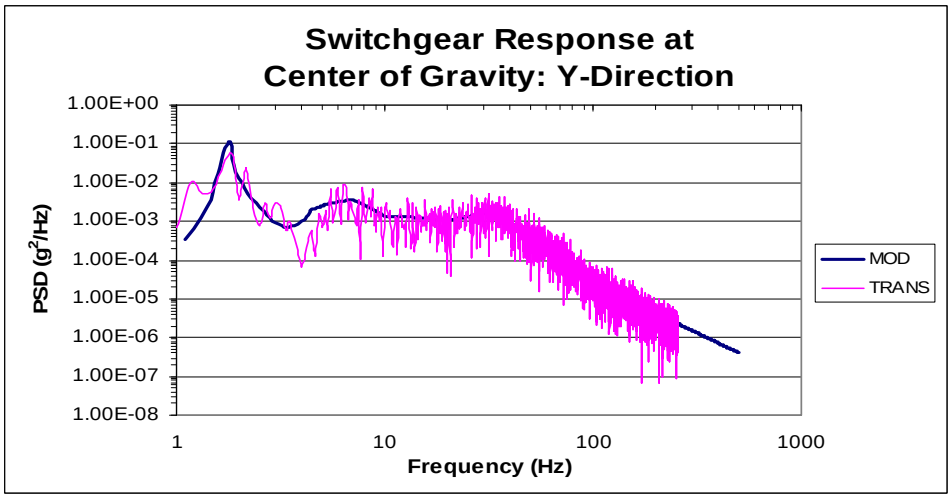

Figure 8: Transient Model vs. Modal Model in Y (0.34 g_{rms})

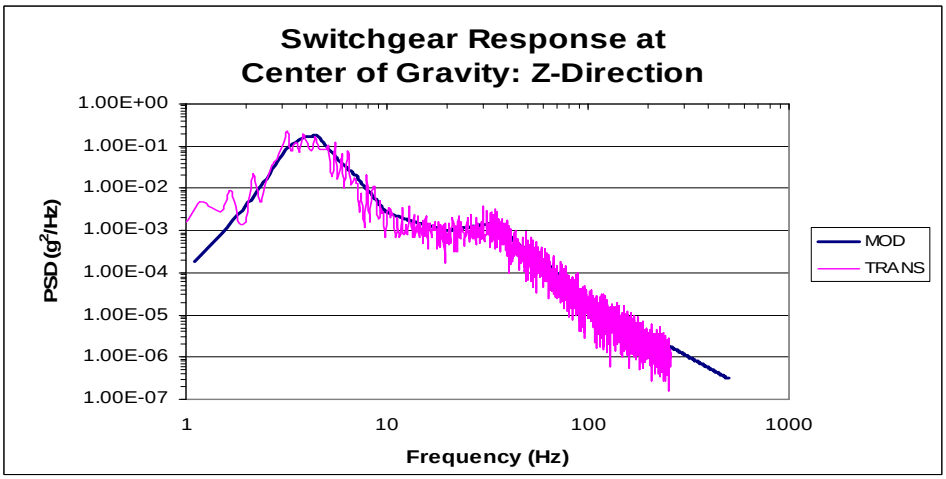

Figure 9: Transient Model vs. Modal Model in Z (0.67 g_{rms})

THE RESULTING SWITCHGEAR ISOLATION SYSTEM INCLUDING RAFT

The final isolation system used 48 coil springs aligned around the cabinet base such that the center of gravity is closely balanced to reduce the amount of coupling between the roll rotation and the Y translation, which is also influenced by the offset of the center of gravity with respect to the center of the isolation mounting plane. This is accomplished by placing 26 springs along the "heavy" side (or front), 20 along the opposing side (back), and one each at each end of the short dimensional side of the cabinet at mid-span. Dampers are placed at each of the four corners at an angle of 35.3° to approach close to equivalent damping in all three translational directions, and also damp the rotational modes. Seven additional dampers are placed internal to the isolation plane as shown in Figure 10.

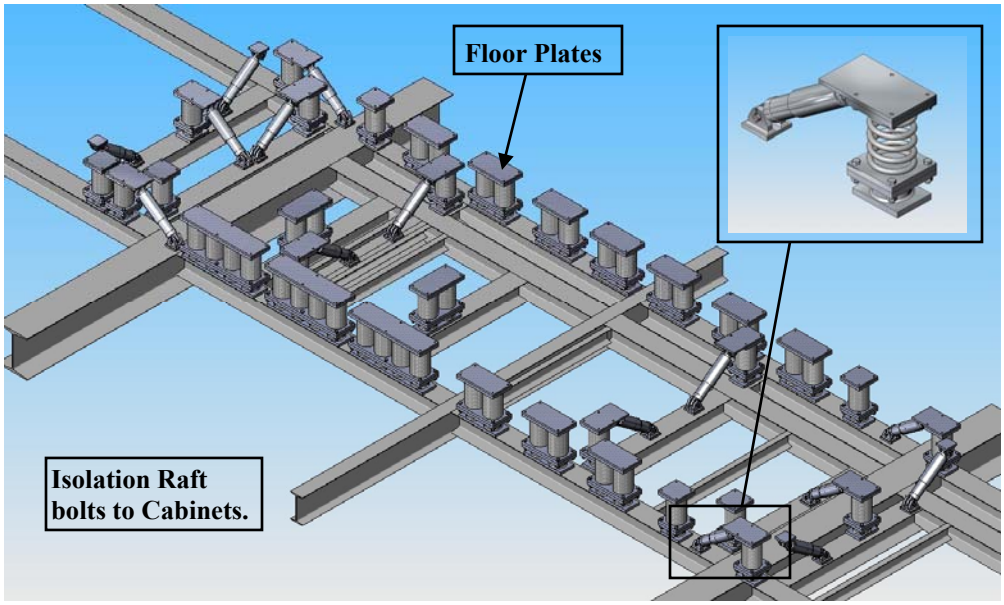

Figure 10: Isometric View of Isolation System

The final spring suspension was based on providing the cabinet a 3.5 Hz fundamental frequency in the vertical direction. This resulted in an individual spring rate of 693 lb/in for each of the 48 springs based on a total system weight of 26,615 lbs. A finite element analysis (FEA) of the coil spring using beam elements was constructed to determine the effective spring rate of the coil springs in their transverse directions. The model was first compared against known accurate software results for model accuracy in determining the vertical spring rate. The results indicated almost identical results between the software and the FEA model, lending confidence to the coil spring FEA model. This in turn was run applying transverse loadings across the spring axes (representative of the horizontal spring rates) with fixed-fixed end conditions. The analysis indicated for this spring design that the transverse spring rate is almost two-thirds of the axial spring rate (485 lb/in). This information was then implemented into the rigid body model. Not considered was the effect of overturning moments on the spring themselves due to their transverse displacement coupled with the static and dynamic compressive loading from a stability standpoint. Also, the effect of changing axial length of the spring on the effective lateral spring rate was not considered.

MEASUREMENTS MADE DURING LAUNCH OF SPACE SHUTTLE

The cabinet response during the launch of STS-115 on September 9, 2006, was monitored by the use of accelerometers to measure the response in all three orthogonal axes at two locations on the cabinet. The input at the base of the cabinet was not captured but is planned to be monitored on a future launch to capture the excitation at the MLP in all three orthogonal axes. Additionally, deflections of the cabinet corners were not captured. Figures 11 through 13 show the captured responses at the cabinet.

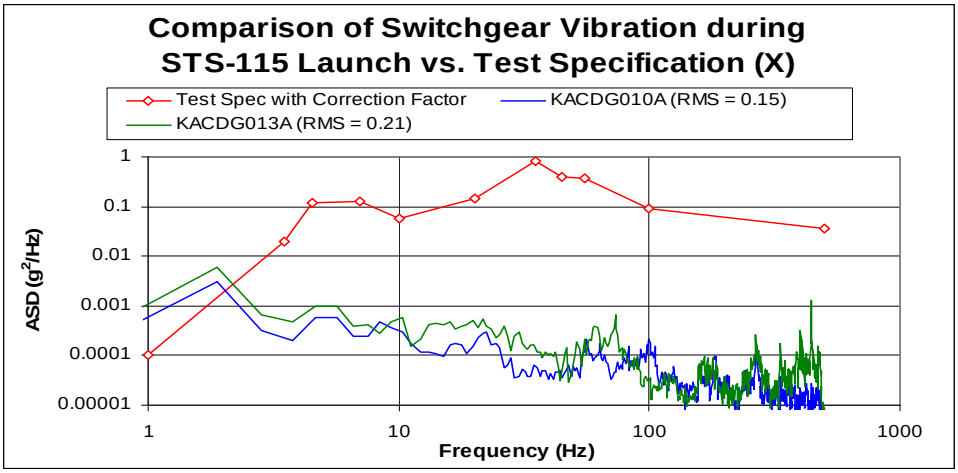

Figure 11: Measured Switchgear Response in X Direction

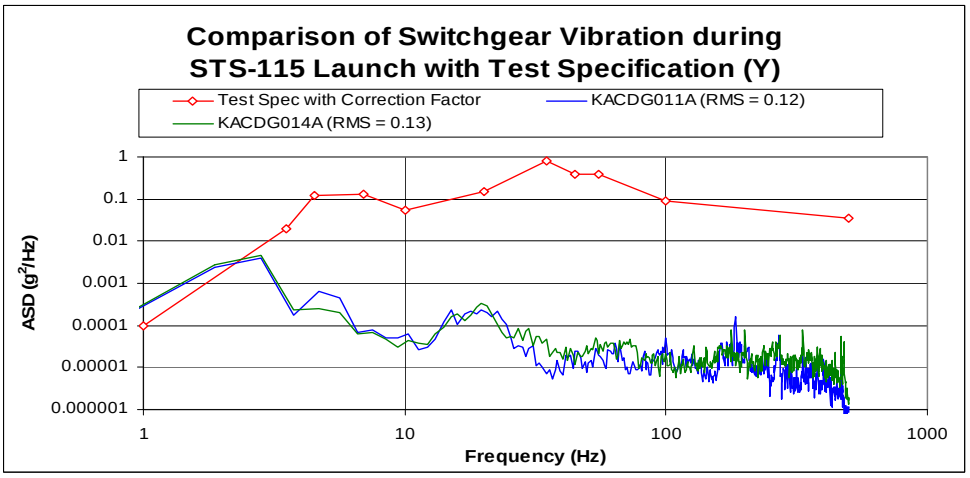

Figure 12: Measured Switchgear Response in Y Direction

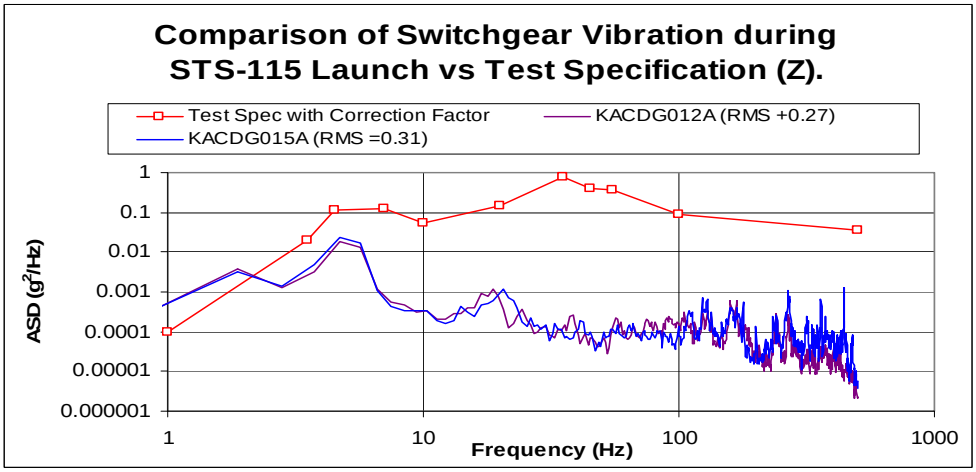

Figure 13: Measured Switchgear Response in Z Direction

As illustrated in the profiles, the higher frequency energy is much less than the input profile provided. This is due to the isolation system both acting as a low pass filter as well as the energy dissipation provided by the dampers. At the very low frequencies, the measurements exceed the input PSD. This is an artifact of the low frequency isolation system and its transference of the energy to the low frequency regime. This is evidenced by the large displacements allowable by the isolators and the resulting travel at the cabinet. The equipment of the cabinet is not sensitive to the low frequency range but rather the higher frequencies in which the energy has been greatly reduced by the isolation system.

Table 3 summarizes the input level, the equipment qualification or fragility levels (maximum input that the equipment is guaranteed to survive), the model results, and the maximum measured response at the cabinet in terms of the g_{rms} levels.

	X	Y	Z
Input Level (g_{rms})	6.82	6.82	6.82
Qualification Level	0.50	0.50	0.50
Model Results	0.34	0.34	0.67
Cabinet Measurements	0.21	0.13	0.31

Table 3: Summary of Input, Qualification, Model, and Measured Results in g_{rms}

- Switchgear base response only provided in the vertical axis
- Switchgear qualification only performed in the horizontal planes due to the nature of the original intent of the switchgear (seismic). The switchgear was believed to be more robust in the vertical direction, but the level was unknown.

The cabinet measurements show a great reduction in the input PSD level at the base as would be expected unless the system was "bottoming" during the launch. Additionally, the resulting responses were well below the cabinet qualification level. There is a slight disparity in the modeling results but this is believed to be due to the assumption that the input was equal in all three axes and the coupling effect of that assumption through the rotational modes to the translational results. In other words, since the actual inputs for modeling purposes are believed to be very conservative for the transverse modes, this caused the predicted response in all three modes to be higher than the actual measurements. However, this results in a higher level of conservatism for the actual system performance over many missions.

CONCLUSIONS

Field measurements of the dynamic response of a cabinet-mounted electronic switchgear made during a recent launch of the Space Shuttle have demonstrated the successful integration of a 6-DOF isolation system consisting of springs and dampers. This has been achieved through the following:

1. Accurately defining the shock and vibration environment that exists.
2. Defining the fragility level of the isolated component through previous component level tests.
3. Analyzing and optimizing the isolation system attributes.
4. Proper design and integration of the isolation system.
5. Field measurement verification.

A video of the cabinet during launch illustrates the effectiveness of the isolation system. Future work involves additional instrumentation during launch to measure the floor acceleration (input) and another series of measurements on the isolated cabinet (response). This will allow the plotting of an actual transmissibility curve and will further demonstrate the benefits of the isolation system.